

# A method to predict the uncompleted climate transition process

Pengcheng Yan<sup>1,3</sup>, Guolin Feng<sup>2</sup>, Wei Hou<sup>2</sup>

[1]{Institute of Arid Meteorology, China Meteorological Administration, Key Laboratory of Arid Climatic Change and Reducing Disaster of Gansu Province, Key Laboratory of Arid Climatic Change and Reducing Disaster of China Meteorological Administration, China}

[2]{National Climate Center, China Meteorological Administration, China}

[3]{China Meteorological Administration Training Center, Beijing, China}

[\*]Correspondence to: Wei Hou (houwei@cma.gov.cn)

## Abstract

Climate change is expressed as a climate system transiting from the initial state to a new state in a short time. The period between the initial state and the new state is defined as transition process, which is the key part to connect the two states. By using a piece-wise function, the transition process is stated approximately (Mudelsee, 2000). However, the dynamic processes are not included in the piece-wise function. Thus, we had proposed a method to study the transition process by using a continuous function. In this manuscript, this method is developed to predict the uncompleted transition process based on the dynamic characteristics of the continuous function. We introduce this prediction method in details and apply it to three ideal time sequences and the Pacific Decadal Oscillation (PDO). The PDO is a long-lived El Niño-like pattern of Pacific climate variability (Barnett et al, 1999). This method reveals a new quantitative relationship during the transition process, which explores a nonlinear relationship between the linear trend and the amplitude (difference) between the initial state and the end state. Since the transition process begins, the initial state and the linear trend are estimated. Then, according to the relationship, the end state and end moment of the uncompleted transition process is predicted.

## Keywords

Prediction method; Transition process of abrupt change; System stability; Pacific

## 1. Introduction

A system transiting from one stable state to another in a short period is called abrupt change (Charney and DeVore, 1979; Lorenz, 1963, 1979). The abrupt change system has two or more states (Goldblatt et al, 2006; Alexander et al, 2012), the system swings between these states that are also called attractors in physics. This phenomena is verified in many fields including biology (Nozaki, 2001), ecology (Osterkamp et al, 2001), climatology (Thom, 1972; Overpeck and Cole, 2006; Yang et al, 2013a, 2013b), brain science (Sherman et al, 1981), etc. The latest observed climate change event is global warming hiatus, which has been studied deeply by many researchers (Amaya et al, 2018; Kosaka and Xie, 2013; Yang et al, 2017). Seven different kind of abrupt changes are mentioned in Thom's research(1972). Over the last several decades, many methods have been proposed to identify different kinds of abrupt change (Li et al, 1996), like Moving T-Test, Cramer's (Wei, 1999), Mann-Kendall (MK, Goossens and Berger, 1986), Fisher (Cabezas and Fath, 2002), etc. It is noticed that most abrupt change detection methods suggests that the abrupt change is around a turning point. The significant difference between the average values of the two sequences on both two sides of the turning point is defined as the index to measure the abrupt change. This kind of detection method has a drawback. It is difficult to detect the abrupt change occurs at the end of sequence.

Mudelsee (2000) studied the abrupt change of a time sequence and illustrated that abrupt change has a duration, which can be quantitatively described with a piece-wise (ramp) function. We developed the detection method by using a continuous function to replace the ramp function( Yan et al, 2014, 2015). The new method can confine the beginning and ending points of abrupt change and quantitatively describes the process of abrupt climate change, and three parameters are introduced. A quantitative relationship among the parameters is revealed (Yan et al, 2015). The relationship could be used to predict the end moment (state) if the system

1 had left the original state but not yet reached to the new state, which is defined as  
2 uncompleted transition process.

3 In this manuscript, three ideal time sequences are tested to study the prediction  
4 method. The prediction method is also applied to study the climate transition process  
5 of the PDO, which is an important signal that reveals climatic variability on the  
6 decadal timescale (Mantua et al, 1997; Barnett et al, 1999; Zhang et al, 1997; Yang et  
7 al, 2004). Previous studies (Lu et al, 2013; Trenberth and Hurrell, 1994) have  
8 indicated that there are many climate changes in the PDO over the past 100 years.  
9 Most researches mentioned the climate changes happened in the 1940s and 1970s.  
10 During the 1940s, the PDO transited from a high state to a low state, while during the  
11 1970s, it did the opposite. All this changes and their processes had been studied in our  
12 previous researches (Yan et al, 2015 2016). The climate transition processes were  
13 explored clearly. However, we still can not know when the transition processes finish  
14 its increasing or decreasing to a stable state if the transition process has begun. We  
15 develop a new method to predict the end state and the end moment of a transition  
16 process based on the quantitative relationship.

## 17 **2. Methods**

### 18 **2.1 The detection method of transition process**

19 The real time sequence changes abruptly as shown in figure 1a, and the system  
20 jumps to a high state in point C. If the period around point C is observed on a shorter  
21 time scale (as shown figure 1b), a transition period is obtained, and it is a part of the  
22 original time sequence. In fact, many abrupt changes could be considered to be a  
23 transition period with a more detailed view. The transition period was expressed with  
24 an ramp function in Mudelsee's research (2000) as shown in figure 1c, and the time  
25 sequence is divided into three segments, including two equilibrium states and one  
26 increasing state. The ramp function is as follows:

$$x_t = \begin{cases} x_1 & t \leq t_1 \\ x_1 + (t - t_1)(x_2 - x_1)/(t_2 - t_1) & t_1 < t \leq t_2 \\ x_2 & t > t_2 \end{cases}, \quad (1)$$

Where  $t$  represents time, and  $x_t$  represent the system states, which is obtained by the linear regression method. It is noted that the climate system is continuous even the sampling sequence that makes it is discontinuous. We used a continuous function to express this transition period approximately, and we also created a novel method to detect the transition period (Yan et al, 2015). Here, the detection method is troduced briefly. The continuous evolution of Logistic model is consistent with the transition process (May, 1976), which is shown in figure 1d. The modified logistic model is expressed as follows:

$$\dot{x} = k(x - u)(v - x), \quad (2)$$

Parameters  $u$  and  $v$  represent the two equilibrium states respectively. Parameter  $k$  represents the switching between different states, and it is defined as instability parameter. As shown in figure 2a, parameters  $u$  and  $v$  being fixed, and setting  $k$  as 0.5, the system transiting to the new state costs a shorter time than that setting  $k$  as 0.4. If parameter  $k$  is set large enough, the system collapses and becomes chaotic ( as shown in figure 2b). When parameter  $k$  is set to different values, more situations have been discussed in detail in the previous research (Yan et al, 2016). The result shows that parameter  $k$  characterizes the stability of the system (the larger the absolute value, the more unstable the system). According to Thom's theory (1972), the system described by a quadratic function would exhibit tipping-point abrupt change, which the system jumps from one state to a new state abruptly. Thus, we did some mathematical derivation to Eq. (2), and the general potential energy is obtained as follows:

$$\begin{aligned} V_{(x)} &= -\int_0^x \ddot{x} dx = -\int_0^x 2k^2 [x - (u + v)/2] (x - u)(x - v) dx \\ &= \frac{k^2}{2} [x^4 - 2(u + v)x^3 + (u^2 + v^2 + 4uv)x^2 - 2(u + v)uvx] \end{aligned} \quad (3)$$

In figure 2c, the potential energy of Eq. (3) is verified to have two states with the lowest energy, and both of them are stable. This bistable structure is common in the

1 climate system (Goldblatt et al, 2006). Therefore, Eq. (2) can be used to describe the  
 2 abrupt change system, and the parameters represent different key factors of the  
 3 transition period during abrupt change. Then, the parameters  $u$ ,  $v$  and  $h$  are obtained  
 4 by regression method (Huang, 1990; Yang et al, 2013a) by using Eq. (4), where  $i$ ,  $x_i$   
 5 denote the time and the state of the system at this time, and  $\bar{i}$ ,  $\bar{x}_i$  are their averages  
 6 respectively. Variable  $n_2$  is the length of second segment. The linear trend  $h$  represents  
 7 the ratio of system state change to time, and it can be expressed by two points on the  
 8 curve approximately as Eq. (5), where the two points are  $A(x_a, t_a)$  and  $B(x_b, t_b)$ .

$$9 \quad \begin{cases} v = \sum_{i=1}^{n_1} x_i / n_1 \\ u = \sum_{i=n_1+n_2+1}^n x_i / n_3 \\ h = \sum_{i=n_1+1}^{n_1+n_2} \bar{i} \cdot \bar{x}_i / \sum_{i=n_1+1}^{n_1+n_2} \bar{i}^2, \end{cases} \quad (4)$$

$$10 \quad h = \frac{x_a - x_b}{t_a - t_b} \quad (5)$$

11 As shown in figure 2d, the transition period during point  $A(x_a, t_a)$  and point  $B(x_b,$   
 12  $t_b)$  is approximately linear. Then, we can use the location parameters  $\alpha$ ,  $\beta$  to express  
 13 system states  $x_a$  and  $x_b$ . By solving Eq. (2), the relationship between  $x$  and  $t$  is  
 14 determined.

$$15 \quad t = \frac{1}{k(u-v)} \ln\left(\frac{x_0-u}{x_0-v} \cdot \frac{x-v}{x-u}\right) + t_0 \quad (6)$$

16 Then, parameter  $h$  is rewritten as Eq. (7). It is noted that the rightmost part is  
 17 only related to the location parameters  $\alpha$  and  $\beta$ , then let it be  $\chi$ . Then, the relationship  
 18 of Eq. (7) is rewritten as Eq. (8).

$$h = \frac{x_b - x_a}{\frac{1}{(\mu - \nu)\kappa} \ln \frac{x_0 - \mu}{x_0 - \nu} \left( \frac{x_b - \nu}{x_b - u} - \frac{x_a - \nu}{x_a - u} \right)}$$

$$= \kappa(\mu - \nu)^2 \frac{(\beta - \alpha)}{\ln \frac{\beta(\alpha - 1)}{\alpha(\beta - 1)}} \quad (7)$$

$$h = \kappa \omega^2 \chi \quad (8)$$

In order to determine the value of parameter  $\chi$ , the relationship among  $\chi$ ,  $\alpha$ ,  $\beta$  is displayed in figure 3b. The dash line in figure 3a is the profile of the diagonal in figure 3b, which represents that the sum of  $\alpha$  and  $\beta$  is 1. Parameter  $\chi$  changes little when the location parameter varies in a certain range as marked with warm color in figure 3b. It means that the closer the points ( $A$  and  $B$ ) are to the middle point, the more significant the linear feature is. Then, the process between point  $A$  and point  $B$  can represent the whole transition process as shown in figure 3c. It is noted that the transition process is symmetrical about the middle point approximately. Thus, we assume that point  $A$  and point  $B$  are symmetrical about the middle point, and the sum of  $\alpha$  and  $\beta$  is 1. The change of parameter  $\chi$  is only related to parameter  $\alpha$  (or parameter  $\beta$ ), as shown in the diagonals in figure 3b (also in figure 3a). Parameter  $\chi$  changes little when parameter  $\alpha$  is about 0.2 or larger. In figure 3c, three different situations are carried out to study the influence of parameter  $\alpha$  on parameter  $\chi$ . In each situation, points ( $A$  and  $B$ ) are set to be different positions, and their parameters were calculated respectively in table 1. The parameters  $\alpha$  are set as 0.20, 0.25, 0.15 respectively in three different situations marked with S1, S2 and S3. For S2 and S3, both of the percentages of  $\alpha$  changing to S1 are 25%, while the percentages of  $\chi$  changing are only 5.15% and 6.76% respectively, which means the percentage change of  $\chi$  is much less than  $\alpha$ . In addition, linear trends of these three ideal models are calculated according to the points and by regression method which are marked as  $h_0$  in table 1. The linear trends are also calculated by the values of point  $A$  and point  $B$  with Eq(5) which are marked as  $h$  in table 1. It is noted that although the positions of points are different, the trend obtained according to the points is almost the same as that

obtained by regression method. The error percentages are 2.36%, 2.25%, 1.38% respectively, which means that when the position of the points (the values of parameters  $\alpha$  and  $\beta$ ) are indefinite, there is little influence on the detection of parameter  $h$ . Thus, in the following sections parameter  $\alpha$  is set as 0.2, and parameter  $\chi$  is 0.2164

## 2.2 The prediction method of transition process

Eq. (8) shows the quantitative relationship among linear trend, instability parameter, and amplitude of change. There is a linear relationship between linear trend and instability parameter; and there is the quadratic function relationship between linear trend and amplitude of change. We did reveal this quantitative relationship much more than in theory but in real time series (Yan et al, 2016). Based on this relationship, we are going to create a new method to deal with the problem that the transition process has not finished. During the real time sequence, the system transits away from the original state, but it has not reached to a new state as shown in figure 4. The red line represents the period which has been experienced, while the gray line represents the period which hasn't been experienced. Based on the system states which is far away from the original state, a quasi linear extension of the transition process is established (dash line). Then the parameters  $v$  and  $h$  are obtained by Eq. (4). Assuming that the parameter  $k$  satisfies the statistics in the history of the system, the parameter  $u$  can be predicted by Eq. (8), and the end moment is also predicted apparently..

$$\begin{cases} x_t = x_{t-1} + kt(x_t - u)(v - x_t) \\ x'_t = x_t + random_t \end{cases}, \quad (9)$$

As shown in figure 5, four ideal time sequences are constructed by using the logistic model and random numbers as Eq. (9). An entire time sequence with 500 moments is shown in figure 5a and three other lengths of time sequences are shown in figures 5b, 5c and 5d respectively. The parameters  $v$ ,  $u$  and  $k$  of the logistic model are set as -1.0, 2.0, 0.1, for the ideal time sequence, and the random number is limited in 0-1. The parameters  $v$ ,  $h$  are obtained by regression method before making prediction.

It has to be noticed that in this ideal time sequence there is just one abrupt change, which means that we have no way to obtain the value of the parameter  $k$  by counting many changes. Thus parameter  $k$  is given directly, and the prediction of the end state (moment) is drawn in figure 5b, 5c and 5d. For the entire time sequence, there are 500 moments as shown in figure 5a. In figure 5b, only 240 moments are given, and the other moments are unknown. Then, we obtain parameters  $v$  and  $h$  by regression method. The parameter  $u$  is calculated with Eq. (8). The blue line represent the prediction result. The transition process would be ended in moment 342 with the end state value 2.92. In figure 5c, the end moment and end state are predicted to be 356 and 2.65 respectively when the time sequence is given 250 moments. In figure 5d, the time sequence is given 260 moments. The end moment and end state are predicted to be 359 and 2.58 respectively. The end moment and the end state of prediction result match the presetting lines. The results also show that the longer the transition process experience, the more accurate the prediction.

### 3. Results

In order to test the validity of this prediction method in a real climate system, we apply this method to predict the uncompleted transition process of the PDO. The PDO index data used is from website of the University of Washington (<http://research.jisao.washington.edu/pdo/>). The time period from January of 1900 to November of 2015 is studied as the training data, and the time period from December of 2015 to April of 2017 is used as the test data. During the following research, a transition process starting from 2011 is studied. According to the prediction method, several parameters have to be determined in advance. We determine parameter  $k$  firstly.

#### 3.1 Threshold of parameter $k$

Parameter  $k$  characterizes the stability of the system during climate change, which means that we can get the value of parameter  $k$  by counting all changes of the



1 PDO index. The histogram in Figure 6a shows the PDO time sequence from January  
 2 of 1900 to November of 2015, and it shows that the PDO went through several  
 3 changes. The green dots in Figure 6a are parameter  $k$  when the sub-sequence length  
 4 takes 20 years. In the early 1940s and late 1970s, there are two transition changes of  
 5 the PDO mainly. The absolute value of the parameter  $k$  is large, which means that the  
 6 system is much more unstable during this two transition changes. In the 1940s, the  
 7 PDO transits from a positive phase to a negative phase, and the  $k < 0$ , whereas the  
 8 situation in the 1970s is the opposite. Figure 6b shows more  $k$  values corresponding to  
 9 the different sub-sequence lengths (as indicated by X-axis, the variation range of the  
 10 sub-sequence is 20-60 years, with an interval of 1 year). The Y-axis is the start  
 11 moment, and the locations of the dots indicate the start moments for the  
 12 corresponding sub-sequence lengths. In particular, the blue dots represent that  
 13 parameter  $k$  is negative, and the red dots represent that it is positive. The dots in the  
 14 left side region are more than the dots in the right side region in figure 6. This is  
 15 because when the length of sub-sequence is short, the amplitude is also often small.  
 16 Therefore, for the entire sub-sequence, there are many transition changes. When the  
 17 length of the sub-sequence reaches or exceeds 50 years, the transition change mainly  
 18 begins in the 1940s and 1970s, which are also investigated in other research (Shi et al,  
 19 2014). The transition changes in these two periods correspond to large  $k$  values, which  
 20 means that these two transition changes are more unstable than others. More statistical  
 21 results indicate that the threshold distribution of parameter  $k$  values in historical  
 22 abrupt change processes exhibit multiple peaks (Figure 7). Specifically, the peak with  
 23 the largest probability is located near to 0. The  $k$  value of the largest peak in the  
 24 distribution is small, which indicates that the abrupt changes that correspond to these  
 25  $k$  values are stable. The  $k$  values also have peaks on the left side and right side of the  
 26 origin. When  $k < 0$ , the PDO time sequence transits from the positive phase to the  
 27 negative phase, when the threshold of the  $k$  peak is wide and the probability is small;  
 28 when  $k > 0$ , the PDO time sequence transits from the negative phase to the positive  
 29 phase, when the threshold of the  $k$  value is narrow and the probability is large. This  
 30 indicates that there are two kind of transitions, which one of them is that the system

1 changes from the positive phase to the negative phase, and the other is that the system  
 2 changes from the negative phase to the positive phase, are not symmetric, and the  
 3 latter is more stable. Because there is a difference in parameter  $k$  when the selected  
 4 sub-sequence length is different, the gray region in the upper right corner of Figure 7  
 5 also shows the statistical properties of parameter  $k$  when the sub-sequence length is 20,  
 6 30, 40, 50, or 60 years. When the length of the sub-sequence is 20 years and 30 years,  
 7 there is only one peak in the distribution of  $k$  values, and the parameter  $k$  value of the  
 8 peak is about 0, which means that the transition change is more stable than the other  
 9 situations. When the length of the sub-sequence is 40, 50, or 60 years, the peak value  
 10 on the side of  $k > 0$  is not considerably different, which indicates that the stability  
 11 degree of the transition change from negative to positive is consistent; the location of  
 12 the peak value on the side of  $k < 0$  moves to the left as the sub-sequence length  
 13 increases, which means that the sub-sequence is longer, the amplitude of detected  
 14 transition change is larger, and it is more unstable. From the perspective of the value,  
 15 a  $k$  value in the range of  $(-10, 10)$  accounts for 80.2% of all  $k$  values, a  $k$  value in the  
 16 range of  $(-5, 5)$  accounts for 74.2%, and a  $k$  value in the range of  $(-2, 2)$  accounts for  
 17 58.6%. In the following studies, the  $k$  value is mainly set in the range of  $(-2, 2)$ .

### 18 **3.2 Values of the initial state $v$ and linear trend $h$**

19 We use the method proposed in section 2.2 to analyze the transition changes of  
 20 the PDO. With different lengths of sub-sequences, three climate changes are detected  
 21 to start from 1976, 2007 and 2011 respectively. In figure 8, the transition changes  
 22 starting from 2007 and 2011 are stated, while the transition change starting from 1976  
 23 has not been shown. In table 2, parameters  $v$  and  $h$  are obtained by regression method  
 24 when the transition change starting from 2007 and 2011. When the length of  
 25 sub-sequence is 20 years or 30 years, only the transition change starting from 2011 is  
 26 detected as shown in figure 8a and figure 8b. The parameter  $v$  is calculated with the  
 27 sequence before 2011 of the entire sub-sequence. Then, the linear trend parameter  $h$  is  
 28 calculated with the segment after 2011 of the entire sub-sequence. For the transition

1 change starting from 2011, the values of initial state were detected to be -0.45 and  
2 -0.03, respectively, and both the linear trends are 1.054/month. When the lengths of  
3 sub-sequences are set as 30 and 40 years, the transition change began in 2007 as  
4 shown in figure 8c and figure 8d, and the values of initial state are 0.36 and 0.41,  
5 respectively, with an linear trend of 0.227/month. Why does the length of the  
6 sub-sequence change and the start moment of the transition process change? When we  
7 detect the transition change in a sub-sequence, the percentile threshold method  
8 (Huang, 1990) is used. Then, a transition change in the sub-sequence is detected  
9 anyway (Yan et al, 2015, 2016). The change with the largest amplitude will be  
10 detected. When the sub-sequence is set to be 10 years, the start moment of the  
11 transition change is identified to be 2011 as shown in table 2.

12 In figure 8, it is noted that the PDO time sequence is leaving the stable state from  
13 the start moment. The transition change experiences a period, which is called as  
14 transition process. When the transition process has not finished, it looks like the  
15 increasing part. In order to detect whether there are other transition change, we  
16 change the length of sub-sequence one year by one year. That is, the sub-sequence  
17 length is set as 10, 11, 12, ..., and 60 years. Then, the initial state  $v$  and the linear trend  
18  $h$  of these transition changes are obtained. In figure 9, the sub-sequence length is set  
19 less than about 40 years, the transition changes are detected only twice. One began in  
20 2007, and the other began in 2011. The value of parameter  $h$  is unchangeable nearly  
21 for each transition change, while the value of parameter  $v$  is changing when the length  
22 of sub-sequence is different. In particular, the abrupt change starting from 2007 is  
23 detected for the sub-sequence of about 30-40 years, and the value of parameter  $v$  is in  
24 the range of (0.28, 0.45). The transition change starting from 2011 is detected for the  
25 sub-sequence of about 10-30 years, and the value of parameter  $v$  increases as the  
26 length of the sub-sequence increases, whereas the variation range of threshold is  
27 (-0.48, 0.12), which is significantly different from the situation of the transition  
28 change starting from 2007.

### 3.3 Prediction of the uncompleted transition change beginning in 2011

After the threshold ranges for parameters  $k$ ,  $v$ , and  $h$  are determined, according to the quantitative relationship, we can calculate the end state and the end moment of the transition process. Using the transition change in 2011 as an example, we study the ending state and end moment for the PDO index transition change. According to the research results that are presented in Sections 3.1 and 3.2, the parameter is  $h=1.054/\text{month}$  in this transition change, and the threshold range of parameter  $k$  is determined to be  $(0, 2)$ . The range of parameter  $v$  is determined to be  $(-0.48, 0.12)$ , and the variation situation of parameter  $u$  and end moment with parameters  $k$  and  $v$  are shown in Figure 10. The results indicate that the threshold range of parameter  $u$  for the ending state is  $(1, 7)$ , and the time range of the ending moment is  $(2013, 2017)$ . According to the probability of parameter  $k$ , the end moment of this transition process is about 2015, and after that time, the sequence stops to increase, approaching to a stable state with value of 1.6.

In figure 11, a sketch map is displayed to explain how the prediction method works briefly. The PDO time sequence is displayed as black line. The period during 2006~2011 is detected as the initial state, and a transition process is increasing from this initial state. It is not able to be known whether the increasing process has been completed or not. Based on the linear regression method, the initial state and the linear trend are obtained and shown as purple dash lines. Then by the method proposed in section 2.2, all possible end states of this transition process are obtained with Eq. (8) as shown in figure 10, and the most likely end state is marked as green dash line.. Unlike the uncompleted transition process of ideal experiment, the transition process has completed in about 2015 since we detected the PDO change in 2016. This transition process started from 2011, and end in 2015. The initial moment and the end moment are marked as black dash lines. However, we are still not sure whether the PDO finish this transition process completely or not for it it appears at the

end of the sequence. As we all know, many statistical methods are not accurate for the detecting both ends of the sequence. Thus, the real PDO sequence during 2016~2017 is added to the end of the PDO time sequence. The PDO value from 2015 to 2017 is almost unchanged, which is consistent with the predicted result.

#### 4. Conclusion and discussion

A novel method had been proposed to identify the transition process of climate change in our previous research. By defining initial state parameter  $v$ , linear trend parameter  $h$ , end state parameter  $u$ , and instability parameter  $k$ , a quantitative relationship among this parameters was revealed. Based on the relationship, we develop a method to study uncompleted transition processes. The method is applied to predict ideal time sequences and the PDO time sequence. In the ideal experiments, three different time sequences with different length are constructed. Based on the initial state and the linear trend which the system had experienced, and the given parameter, the end state and end moment of the transition process are predicted. The prediction result does match the ideal time sequence well. For the PDO time sequence, a transition change began in 2011 was taken to test the prediction method. The end moment of this transition process is predicted to be 2015. which is consistent with the real time sequence.

In this prediction method, the quantitative relationship among the parameters characterizing the transition process is vital. Accord to the segment of the transition process which has been happened, we determine the parameters. Then, we predict the end moment and the end state. In fact, this is also a extrapolation method. However, if the transition process has not begun, we can not predict this climate change. There is no other statistical method that can predict the climate change which has not occurred only by time sequence. It is noted that the uncompleted climate change we studied is closed to the end of the sequence. Due to the lake of enough data, it is difficult to study the end of time sequence by using other statistical methods.

## Acknowledgements

We thank two anonymous reviewers for their valuable suggestions. This study was jointly sponsored by National Key Research and Development Program of China (Grant No. 2018YFE0109600), National Natural Science Foundation of China (Grant Nos. 41875096, 41775078, 41675092), Meteorological scientific research project of Gansu Meteorological Bureau (MS201914).

## References

- Alexander R, Reinhard C, Andrey G. Multistability and critical thresholds of the Greenland ice sheet. *Nature Climate Change* 2012; 429-432
- Amaya D, Siler N, Xie S, Miller A. The interplay of internal and forced modes of Hadley Cell expansion: lessons from the global warming hiatus. *Climate Dyn* 2018; 51, 305–319, doi:10.1007/s00382-017-3921-5
- Barnett TP, Pierce DW, Latif M. et al. Interdecadal interactions between the tropics and midlatitudes in the Pacific basin. *Geophys. Res. Lett.*, 1999, 26: 615-618.
- Cabezas H, Fath BD. Towards a theory of sustainable systems. *Fluid Phase Equilibria* 2002; 194–197 3, doi:10.1016/S0378-3812 (01)00677-X
- Charney JG, DeVore JG. Multiple flow equilibria in the atmosphere and blocking, *J. Atmos. Sci* 1979; 36, 1205–1216, doi: 10.1175/1520-0469 (1979)0362.0.CO;2
- Goldblatt C, Lenton TM, Watson AJ. Bistability of atmospheric oxygen and the Great Oxidation. *Nature* 2006; 443:683-686, doi: 10.1038/nature05169
- Goossens C, Berger A. Annual and Seasonal Climatic Variations over the Northern Hemisphere and Europe during the Last Century. *Annals of Geophysics* 1986; 4: 385, doi: 10.1016/0040-1951 (86)90317-3
- Huang JY. *Meteorological Statistical Analysis and Prediction*, Beijing: China Meteorological Press 1990; 28–30
- Kosaka Y, Xie SP. Recent global-warming hiatus tied to equatorial Pacific surface cooling. *Nature* 2013; 501: 403–407, doi: 10.1038/nature12534
- Li JP, Chou JF, Shi JE. Complete detection and types of abrupt climatic change. *Journal of Beijing Meteorological college* 1996; 1:7-12
- Liu TZ, Rong PPg, Liu SD, Zheng ZG, Liu SK. Wavelet analysis of climate jump. *Acta Geophysica Sinica* 1995; 38 (2):158-162
- Lorenz EN. Deterministic nonperiodic flow. *J. Atmos. Sci* 1963; 20:130, doi: 10.1175/1520-0469 (1963)020<0130:DNF>2.0.CO;2
- Lorenz EN. Nondeterministic theories of climatic change. *Quaternary Research* 1976; 6 (4):495-506, doi:

1 10.1016/0033-5894 (76)90022-3

2 Lu CH, Guan ZY, Li YH, Bai YY. Interdecadal linkages between Pacific decadal oscillation and interhemispheric  
3 oscillation and their possible connections with East Asian Monsoon. *Chinese J. Geophys* 2013; 56 (4):1084-1094,  
4 doi: 10.1002/cjg2.20012

5 Mantua NJ, Hare S, Zhang Y, John W, Robert F. A Pacific Interdecadal Climate Oscillation with Impacts on  
6 Salmon Production PDO. *Bull.amer.meteor.soc* 1997; 78 (6):1069-1079, doi; 10.1175/1520-0477  
7 (1997)078<1069:APICOW>2.0.CO;2

8 May RM. Simple mathematical models with very complicated dynamics. *Nature* 1976, 261:459–467, doi:  
9 10.1201/9780203734636-5

10 Mudelsee M. Ramp function regression: a tool for quantifying climate Transitions, *Comput. Geosci* 2000,  
11 26:293–307, 10.1016/s0098-3004 (99)00141-7

12 Nozaki K. Abrupt change in primary productivity in a littoral zone of Lake Biwa with the development of a  
13 filamentous green-algal community[J]. *Freshwater Biology*, 2001, 46(5):587-602.

14 Newman M, Alexander MA, Ault TR, Cobb KM. The Pacific Decadal Oscillation, Revisited. *J. Climate* 2016; 29:  
15 4399–4427, doi: 10.1175/JCLI-D-15-0508.1

16 Osterkamp S, Kraft D, Schirmer M. Climate change and the ecology of the Weser estuary region: Assessing the  
17 impact of an abrupt change in climate[J]. *Climate Research*, 2001, 18(1):97-104.

18 Overpeck JT, Cole JE. Abrupt change in earth's climate system. *Annu. Rev. Environ. Resour* 2006; 31:1-31 doi:  
19 10.1146/annurev.energy.30.050504.144308

20 Sherman DG, Hart RG, Easton JD. Abrupt change in head position and cerebral infarction. *Stroke* 1981; 12 (1):2,  
21 doi: 10.1161/01.STR.12.1.2

22 Shi WJ, Tao FL, Liu JY, Xu XL, Kuang WH, Dong JW, Shi XL. Has climate change driven spatio-temporal  
23 changes of cropland in northern China since the 1970s? *Climatic Change* 2014; 124:163-177, doi:  
24 10.1007/s10584-014-1088-1

25 Thom R. *Stability Structural and Morphogenesis*. Sichuan:Sichuan Education Press, 1972

26 Trenberth KE, Hurrell JW. Decadal atmosphere-ocean variations in the Pacific. *Clim. Dyn* 1994; 9:303-319, doi:  
27 10.1007/BF00204745

28 Wei FY. *Modern Climatic Statistical Diagnosis and Forecasting Technology*, eijing: China Meteorological Press,  
29 1999

30 Yan PC, Feng GL, Hou W, Wu H Statistical characteristics on decadal abrupt change process of time sequence in  
31 500 hPa temperature field. *Chinese Journal of Atmospheric Sciences* 2014; 38 (5): 861–873

32 Yan PC, Feng GL, Hou W. A novel method for analyzing the process of abrupt climate change. *Nonlinear*  
33 *Processes in Geophysics* 2015; 22:249-258, doi: 10.5194/npg-22-249-2015

34 Yan PC, Hou W, Feng GL Transition process of abrupt climate change based on global sea surface temperature  
35 over the past century, *Nonlinear Processes in Geophysics* 2016; 23:115–126, doi:10.5194/npg-23-115-2016

36 Yang XQ, Zhu YM, Xie Q, Ren XJ. Advances in studies of Pacific Decadal Oscillation. *Chinese Journal of*

1 Atmospheric Sciences 2004; 28 (6):979-992

2 Yang P, Xiao ZN, Yang J, et al. Characteristics of clustering extreme drought events in China during 1961–2010.

3 Acta Meteorologica Sinica, 2013a, 27(2):186-198.

4 Yang P, Ren GY, Liu W. Spatial and temporal characteristics of Beijing urban heat island intensity. Journal of

5 applied meteorology and climatology, 2013b, 52(8):1803-1816.

6 Yang P, Ren GY, Yan PC. Evidence for a strong association of short-duration intense rainfall with urbanization in

7 the Beijing urban area. Journal of Climate, 2017, 30(15):5851-5870.

8 Zhang YJ, Wallace M, Battisti DS. ENSO-like interdecadal variability :1900-93. J .Climate 1997; 10:1004-1020,

9 doi: 10.1175/1520-0442 (1997)010<1004:ELIV>2.0.CO;2

10

11



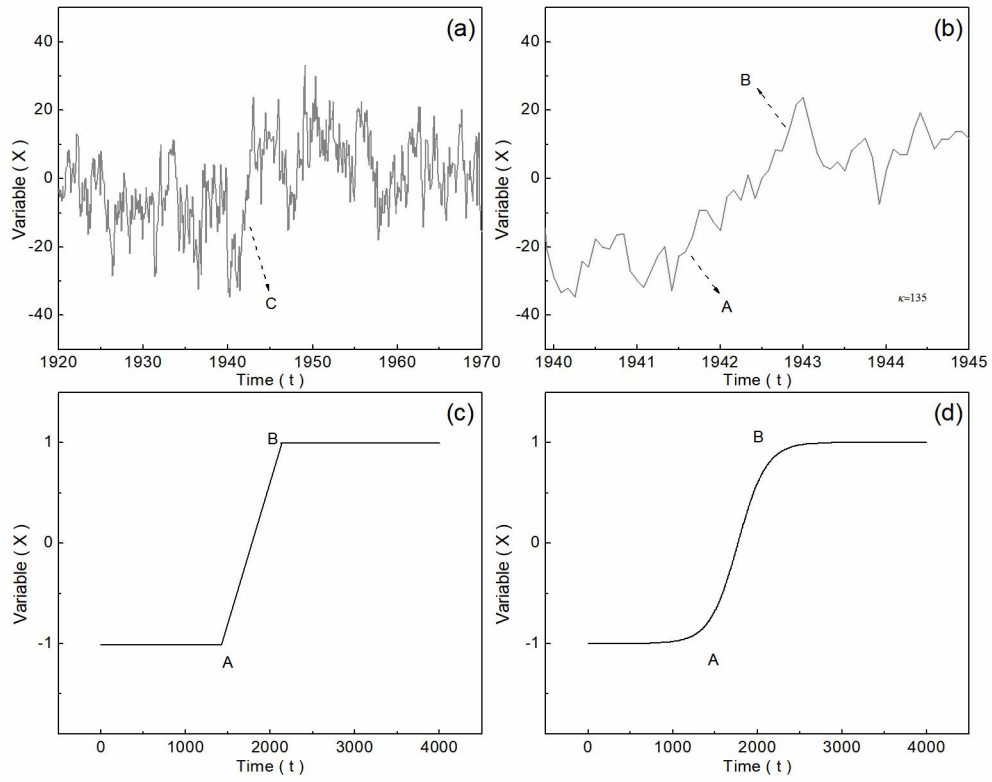
1 Table1. The parameters of ideal models

Situations	$\alpha$	$\chi$	$h0$	$h$	$ h0-h /h$
S1	0.20	21.64E-2	12.99E-4	12.69E-4	2.36%
S2	0.25	22.76E-2	9.10E-4	8.90E-4	2.25%
S3	0.15	20.18E-2	32.27E-4	32.72E-4	1.38%

2 Table2. Parameters  $\nu$  and  $h$  obtained with different sub-sequences

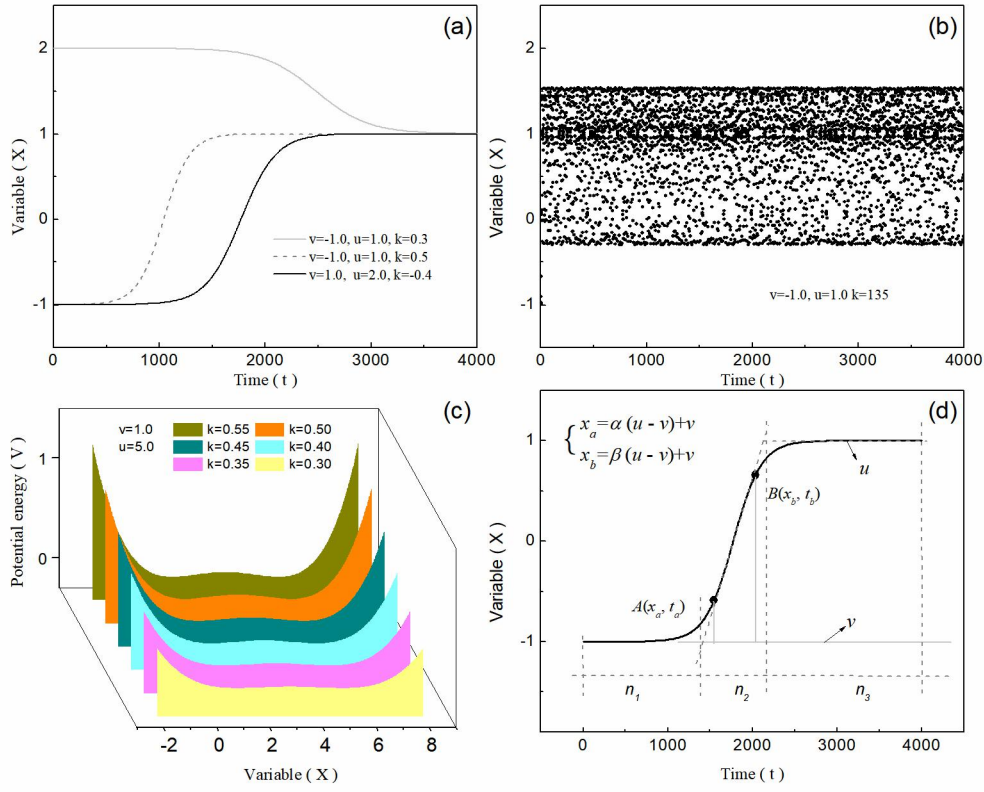
Length of sub-sequence	Start moment (year.month)	$\nu$	$h$ (month <sup>-1</sup> )
10a	2011.06	-0.45	1.054
20a	2011.06	-0.03	1.054
30a	2007.11	0.36	0.227
40a	2007.11	0.41	0.227

3



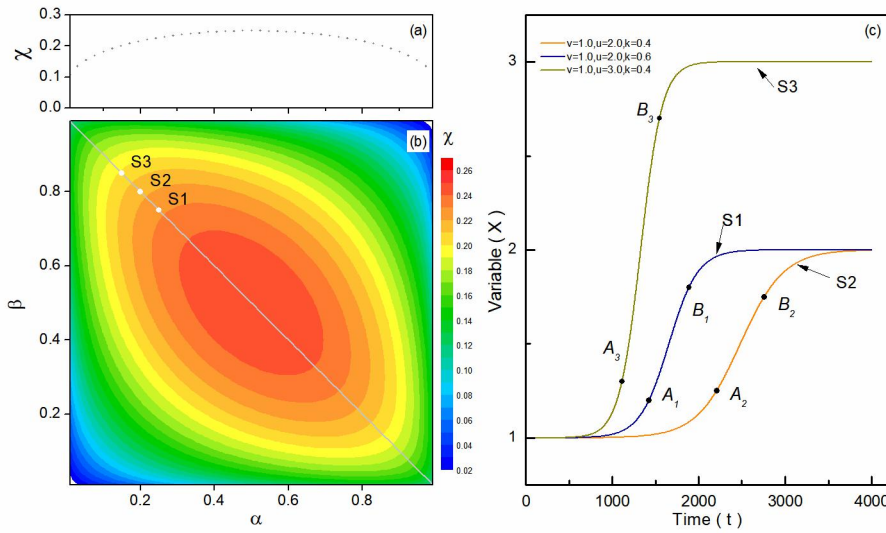
1

2 Figure 1. Transition process of abrupt change in real time sequence and ideal time  
 3 sequence. (a) The PDO time sequence during 1920 to 1970; (b) The PDO time  
 4 sequence during 1940 to 1945; (c) The transition process presented by piece-wise  
 5 function; (d) The transition process presented by continuous function



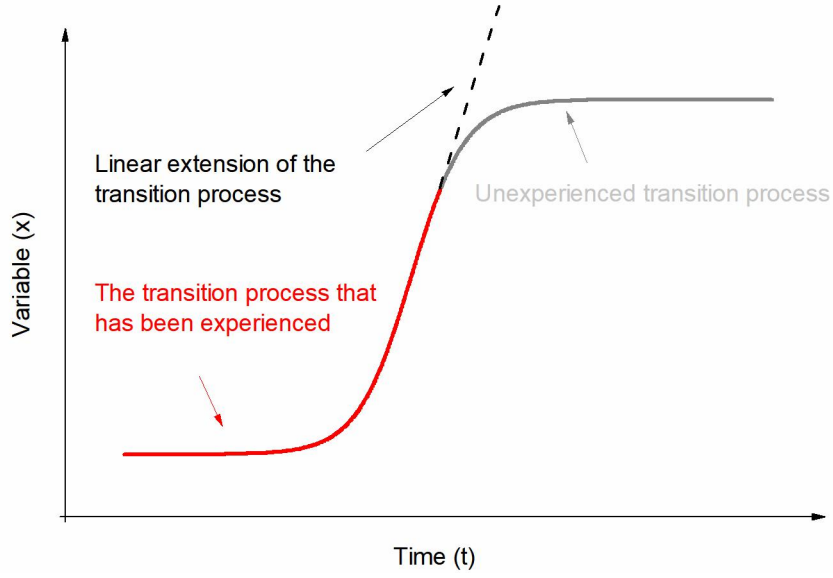
1

2 Figure 2. The system presented by Eq. (2). (a)The transition processes of system  
 3 swinging between different stable states since the parameters are different; (b)The  
 4 system stays in unstable states; (c)The generalized potential energy function of system  
 5 performs differently since the parameters are different; (d)Different segments of the  
 6 transition process in the ideal time sequence and the system states  $x$  expressed with  
 7 location parameters.



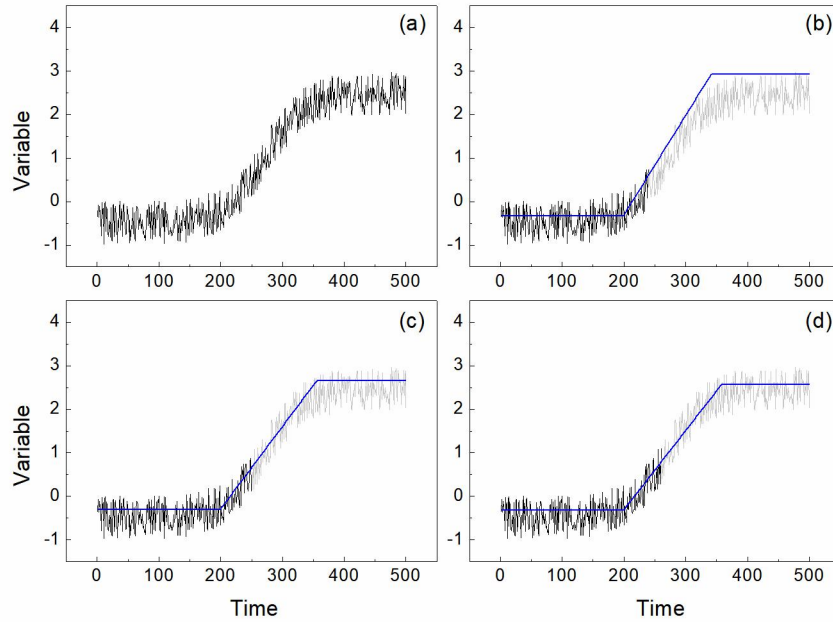
8

- 1 Figure 3. The influence of different value of parameters  $\alpha$  and  $\beta$  on parameter  $\chi$  and  
2 parameter  $h$ . (a) Diagonal section of parameter  $\chi$  in figure b (gray line); (b) Parameter  
3  $\chi$  with location parameters  $\alpha$  and  $\beta$ ; (c) Points  $A$  and  $B$  stay in different positions in  
4 three situations marked as S1, S2, S3.



5

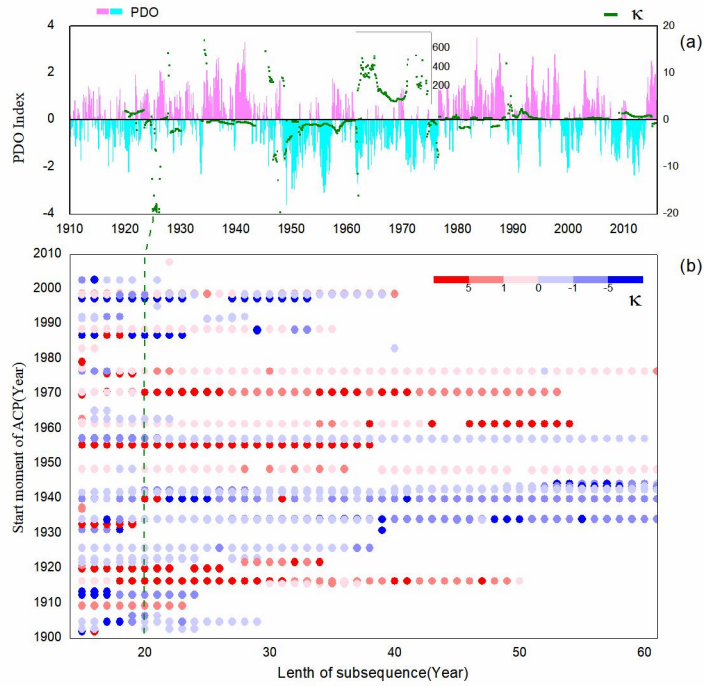
- 6 Figure 4. The schematic diagram of prediction method.



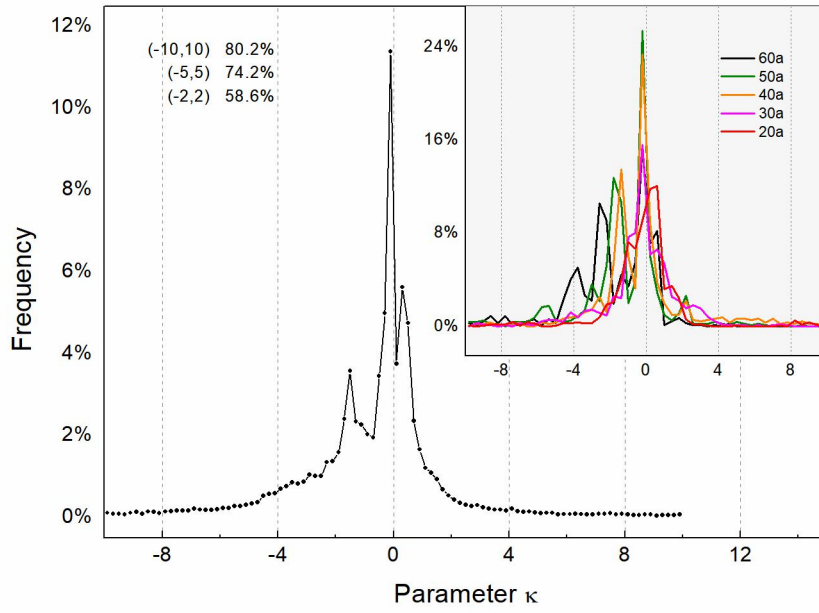
7

- 8 Figure5. The ideal time sequence constructed by the logistic model and random  
9 numbers. (a) Completed transition process with 500 moments, Uncompleted transition  
10 processes (the gray lines) and their prediction result (the blue lines) with (b) 240

1 moments, (c) 250 moments, and (d) 260 moments, the light gray lines are the original  
 2 entire ideal time sequences.

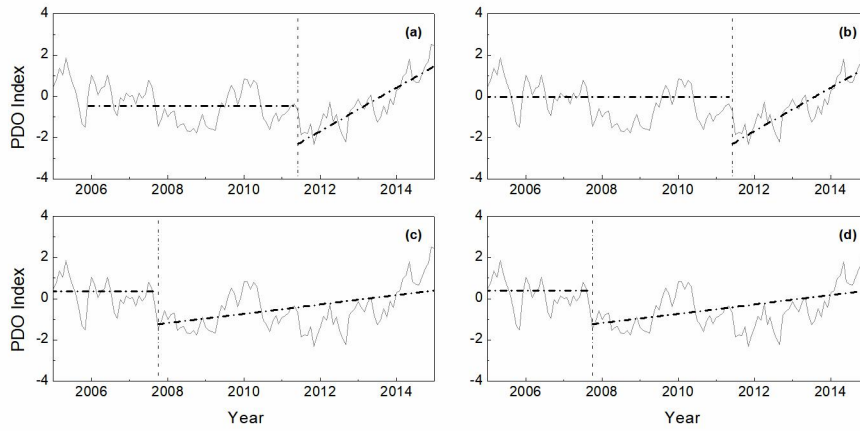


3  
 4 Figure 6. Identification of the PDO time sequence and instability parameter k with  
 5 different sub-sequence lengths. (a) The X-axis is the year, the histogram in the figure  
 6 shows the PDO time sequence (left panel), and the green dots indicate the value of  
 7 parameter k when the sub-sequence is 20 years (right panel); (b) the start moments of  
 8 transition changes with different sub-sequence lengths (the red color dots represent  
 9 increasing changes, and blue color dots represent decreasing changes, with deeper  
 10 colors representing higher values). The X-axis is the sub-sequence length (month),  
 11 and the Y-axis is the start moment of abrupt change (year).



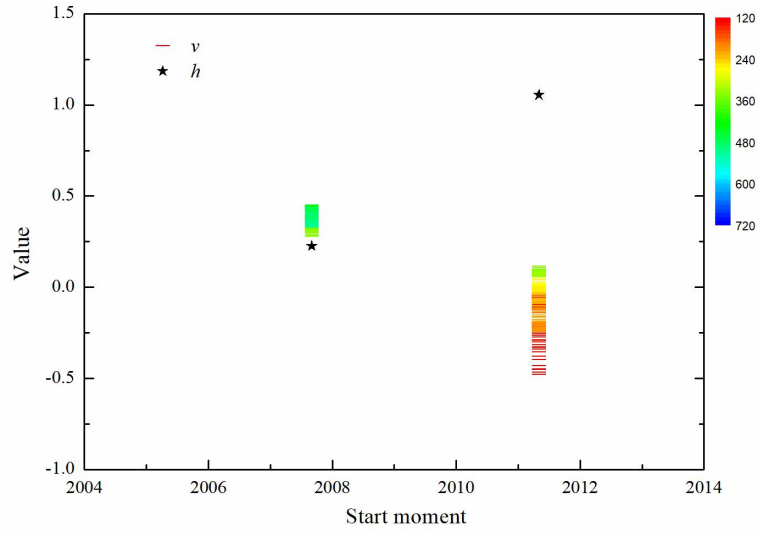
1

2 Figure 7. Statistical results of instability parameters for different sub-sequence lengths.  
 3 The X-axis is the value of the parameter, and the Y-axis is the statistical frequency  
 4 with a sub-sequence length of 10 years. The gray region in the upper-right corner is  
 5 for the sub-sequence of 20-60 years.



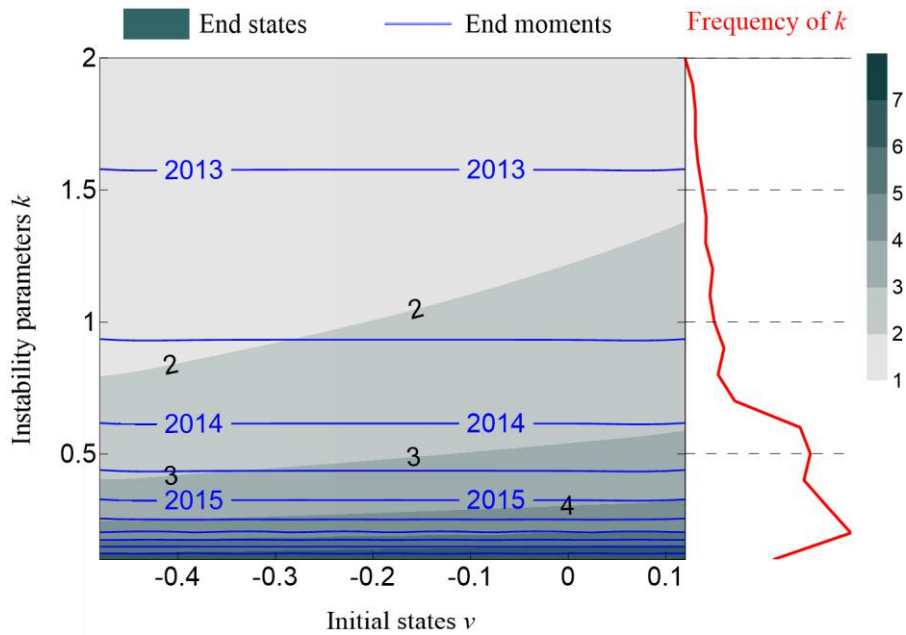
6

7 Figure 8. The PDO time sequences and the detection of parameters  $\nu$  and  $h$  when the  
 8 sub-sequence was set as (a)10 years, (b)20 years, (c)30 years, (d)40 years. The gray  
 9 lines is PDO time sequences. The horizontal dash lines represent initial states, the  
 10 slope dash lines represent linear trend lines of transition change, and vertical dotted  
 11 line represent the start moment.



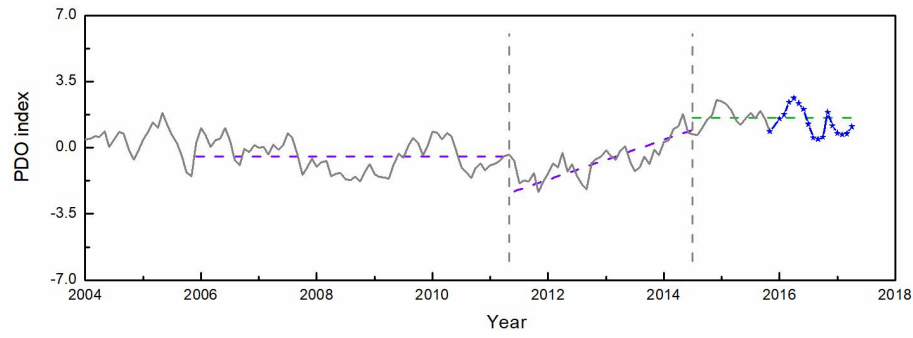
1

2 Figure 9. The values of the parameters  $v$  and  $k$  of two transition changes with different  
3 lengths of sub-sequence. The black stars represent the values of parameter  $h$ , and the  
4 colourful short bar represent the values of parameter  $v$ . The colour bar represents the  
5 sub-sequence length.



6

7 Figure 10. Variation end state and end moment with the initial state parameter  $v$   
8 (horizontal ordinate) and instability parameter  $k$  (vertical coordinate). The red line on  
9 the right side shows the probability distribution of instability parameter  $k$ .



1

2 Figure 11. Prediction of the PDO index. The gray line is the PDO index before 2015;  
 3 the line with starts is the PDO index after 2015; the gray dash line represent the start  
 4 moment; the purple dash lines represent the initial state and the linear trend line, the  
 5 green line represent the prediction end state.